Macro-Scale Hydrologic Model Implementation

Marketa M Elsner[1]

Alan Hamlet[1,2]

[1] Center for Science of the Earth System, Climate Impacts Group, University of Washington

[2] Dept of Civil and Environmental Engineering, University of Washington

1. Introduction

In recent years the impacts of climate change on water resources in the Pacific Northwest (PNW) has been widely recognized (Chapter 1, this report). Approaches that couple downscaled climate scenarios (Chapter 2, this report) to a physically based hydrologic model have provided an effective means of assessing the impacts of global climate change on hydrology (e.g. Elsner *et al*. 2010), water resources systems (e.g. Hamlet *et al.* 2010; Vano *et al.* 2010), and the natural environment (e.g. Littell *et al.* 2010). In these studies the hydrologic model functions as a "translator" between changes in climate and hydrologic changes such as loss of snowpack, altered streamflow timing, changing evaporation, etc.

The Variable Infiltration Capacity (VIC) macro-scale hydrologic model used in this study has been applied to assess the impact of climate change on hydrology of the Columbia River (CRB) basin in a number of previous studies. The Intergovernmental Panel on Climate Change (IPCC) produces an assessment of the state of climate change science approximately every 7 years and as part of the assessment, climate change scenarios from global climate models (GCMs) are published for use by researchers to conduct their own regional assessments. Hamlet and Lettenmaier (1999) studied the implications of GCM projections from the second IPCC assessment (1995) over the Columbia River Basin. Following the third IPCC Assessment Report (2001), Payne *et al.* (2004) studied climate change effects on the Columbia River Basin. Lee *et al.* (2009) explored the effects of projected hydrologic change on flood control operations. All of the above studies employed VIC implementations at $1/8^{th}$ degree (latitude/longitude) resolution.

Such studies have succeeded in providing useful climate change scenarios for large-scale planning in the basin, but have limited ability to accurately resolve smaller sub-basins of interest to other stakeholders (Chapter 1, 2, 8, this report). To better resolve smaller watersheds, we have implemented the VIC hydrologic model at $1/16^{th}$ degree latitude by longitude resolution across the CRB (approximately $30km^2$ or 7400

acres per cell), extending the VIC model developed for the Washington State Climate Change Impacts Assessment (Elsner *et al*. 2010). In addition to the macro-scale VIC implementation, a fine-scale hydrologic implementation using the Distributed Hydrology Soil Vegetation Model (DHSVM) has been carried out at 150m resolution over 5 pilot watersheds that cover a range of terrain and climatic conditions within the CRB (Chapter 6, this report).

This chapter describes the macro-scale VIC model, implementation and model calibration procedures, and evaluation of the macro-scale hydrologic scenarios which form the basis for the core hydrologic data bases produced for this study (see Chapter 8, this report). The fine scale hydrologic model implementation is described in Chapter 6 (this report).

2. Approach/Methods

The methods outlined in this section incorporate a number of important improvements in the macro scale hydrologic model and its implementation. The most important of these changes is the increased spatial resolution of the VIC hydrologic model and recalibration of this model over the entire CRB. Important changes in the downscaling procedures used to translate GCM simulations to driving data for the hydrologic models have also been made (See Chapter 4 on GCM Downscaling Methods and Applications). An historical input data set including daily precipitation, maximum and minimum daily temperature, and windspeed was developed for this study at 1/16th degree spatial resolution and its unique features are described in Chapter 3 on historic meteorological driving data.

The comprehensive hydrologic databases produced for the entire CRB (Chapter 8, this report) are based upon simulations using the VIC macro-scale hydrologic model (Liang *et al*. 1996; Liang *et al*. 1998; Nijssen *et al*. 1997) implemented at 1/16th degree resolution. This implementation allows for a more accurate rendering of topographic features and the sensitivity of smaller watersheds to changes in climate forcing. The current VIC implementation extends the 1/16th degree VIC implementation developed for

the WACCIA (Elsner *et al*. 2010). While Elsner *et al.* (2010) primarily used model parameters calibrated at the 1/8th degree scale and applied them at 1/16th degree, here we follow the approach of Matheussen *et al.* 2000 to calibrate 12 large watersheds in the CRB at the 1/16th degree scale (see Figure 1). Further model evaluation at smaller watershed scales has been conducted for streamflow locations for which naturalized flow data was available. Further details of the calibration approach are provided in Section 1.5. Further details of the statistical bias correction approach are provided in Chapter 8 on data products.

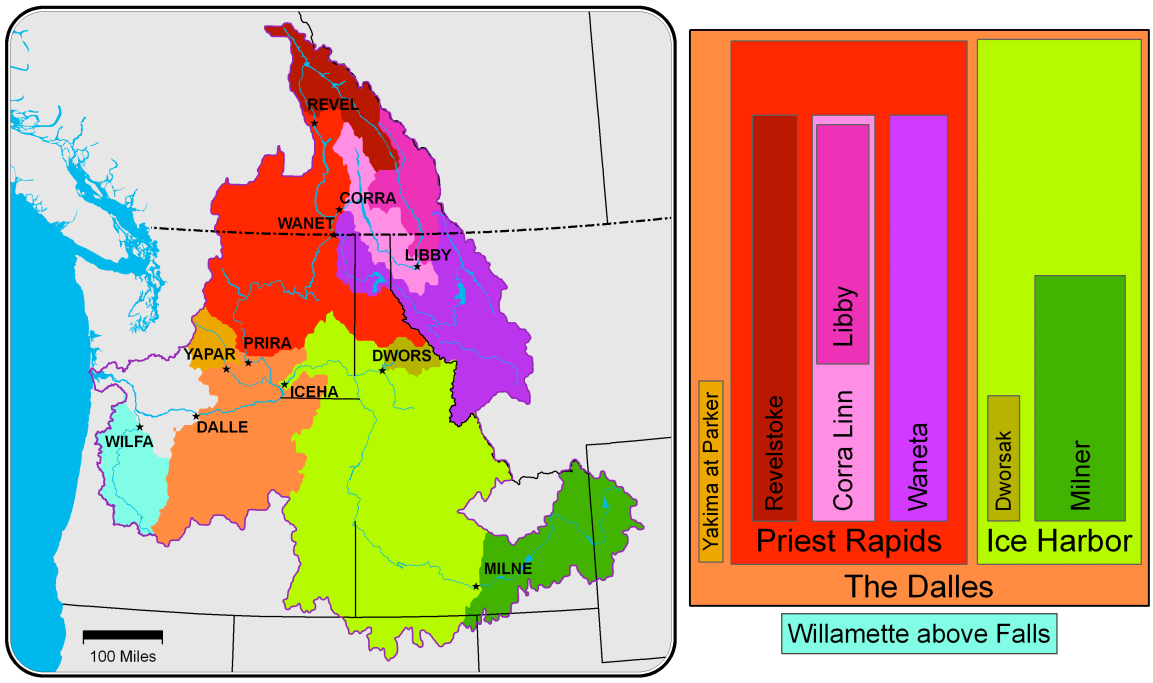

Figure 1 Overview map of Columbia River watershed and coastal drainages to Washington and Oregon.

2.1 Overview of the Variable Infiltration Capacity Model

The VIC model (Liang *et al*. 1994; Liang *et al.* 1996; Nijssen *et al.* 1997) is a spatially distributed hydrologic model that solves the water balance at each model grid cell (see Figure 2 for diagram). Its initial purpose was to serve as a land surface model incorporated dynamically in a global climate model which would more accurately simulate land processes that a GCM cannot explicitly resolve. For off line studies (i.e. when not incorporated in a climate model) the model can also be run in "water balance" mode, in which case the surface temperature is assumed to be equal to the air

temperature. This approach reduces computational requirements, and has been frequently used for water resources studies like this one. At 1/16th degree resolution, the VIC model is most appropriately applied at spatial resolutions of about 500km^2 or greater (193 mi^2), which equals approximately 15 model grid cells.

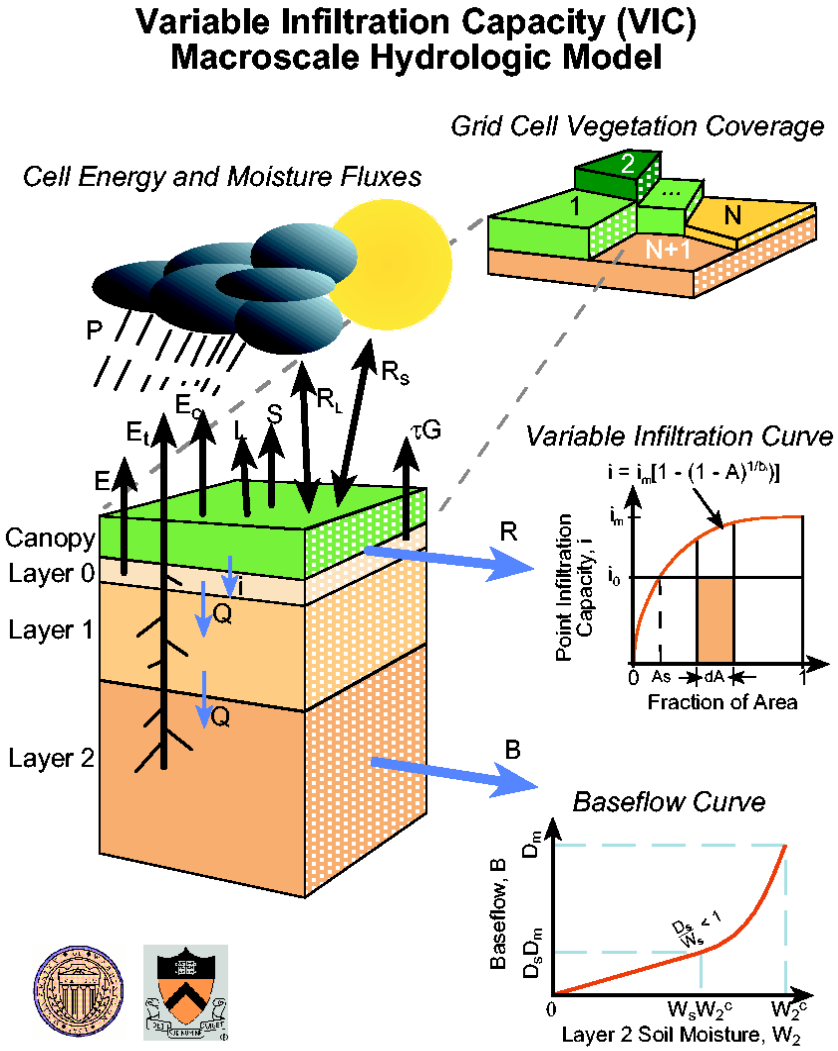

Figure 2 VIC model overview

As implemented here (offline, water balance mode), VIC is driven by daily inputs of precipitation, maximum and minimum air temperature, and windspeed (Chapter 3). Additional model forcings that drive the water balance, such as solar (short-wave) and long-wave radiation, relative humidity, vapor pressure and vapor pressure deficit, are

calculated in a preprocessing step within the model. What makes the VIC model unique is its representation of the soil column and parameterization of the infiltration process, which impacts the vertical distribution of soil moisture in the model grid cell. The VIC model represents multiple vegetation types and 3 soil layers which allows for variable infiltration and evaporation. Potential evapotranspiration is calculated using a Penman Monteith approach (Maidment *et al.* 1993). VIC also contains a sub-daily (1-hour time step) snow model which follows the algorithm of Cherkauer and Lettenmaier 2003, Wigmosta *et al*. 1994, and Andreadis *et al*. 2009.

Subgrid elevation bands increase the ability to resolve snow processes within each grid cell. For the current application, an elevation band resolution of approximately 500m is imposed (less than 5 elevation bands in even the steepest locations). For each grid cell, the model calculates water balance variables (among others) such as evapotranspiration, runoff, baseflow, soil moisture, and snow water equivalent. A full list of output variables for this study is provided in Chapters 4 and 8. To calculate streamflow in larger basins, daily runoff and baseflow are used as input to an offline routing model (based on Lohmann *et al.* 1996).

Elsner *et al.* (2010) added additional calculations in the model to allow output of daily potential evapotranspiration (PET) for each model grid cell. PET is the amount of water that would be transpired by vegetation, provided unlimited water supply, and is often used as a reference value of land surface water stress in characterizations of climate interactions with forest processes (e.g., Littell *et al*. 2010). PET is calculated in the VIC model using the Penman-Montieth approach (Liang *et al*. 1996) and the user may choose to output PET of natural vegetation, open water, and PET of certain reference agricultural crops.

These types of PET differ by the assumptions made in the Penman Monteith equation. Generally, the Penman Monteith equation requires information including solar radiation, air temperature, windspeed, as well as vegetation characteristics such as leaf area index (LAI), aerodynamic resistance and vegetation resistances, including

architectural and canopy resistance. PET values differ in their assumptions of albedo, LAI, aerodynamic resistance and vegetation resistances. Table 1 summarizes the differences in these variables and they are further described below. For all PET types, windspeed height is fixed at heights well above vegetation. Also, aerodynamic resistance is dependent on vegetation type, so for reference crop PET, aerodynamic resistances are fixed for these crop types.

Table 1 Summary of potential evapotranspiration variables and assumptions in their calculation.

PET variable	Albedo	Vegetation Resistence
PET1 (natural vegetation, no water limit)	Varies by vegetation type and month	Rs, Rarc, Rc, LAI varies by vegetation type
PET2 (open water surface - fixed albedo)	0.1	Rs=0 s/m Rarc=0 s/m LAI varies by vegetation type
PET3 (natural vegetation, no water limit, no vegetation resistance)	Varies by vegetation type and month	Rs=0 s/m Rarc=0 s/m Rc=0 s/m LAI = 1.0
PET4 (Tall reference crop – alfalfa)	0.23	Rs = 100 s/m Rarc = 25 s/m LAI = 4.45
PET5 (Short reference crop - short grass)	0.23	Rs = 100 s/m Rarc = 25 s/m LAI = 2.88

Natural vegetation PET (PET1) assumes the albedo, vegetative resistance, and aerodynamic resistances of natural vegetation, as if the vegetation is in place as is, and the plant evapotranspiration is not limited by water supply. The windspeed height is defined as the sum of the wind height, displacement, roughness, and 10 meters (default used so windspeed height is adequately high above vegetation).

Open water evapotranspiration (PET2) is similar to pan evaporation that is often recorded at reservoirs. This variable assumes that the albedo, or fraction of light that is reflected from the surface, is 0.1. The aerodynamic resistance is set equal to that of a short reference crop. The vegetative resistances (stomatal and architectural) are set to zero. It appropriate only to evaluate this variable during summer months when open

water would not be frozen and snow-covered, as this causes some of the assumptions in this calculation to be invalid.

Short reference crop PET (PET5) is the PET assuming the only present vegetation type is grass. The height of grass is set to 0.12 meters. The albedo for grass is assumed to be 0.23. The vegetation resistance is assumed to be 100 s/m for stomatal resistance and 25 s/m for architectural resistance s/m.

Tall reference crop PET (PET4) is the PET assuming the only present vegetation type is alfalfa. The height of alfalfa is set to 0.5 meters. The albedo, resistance factors, and windspeed height are assumed to be the same as for the short reference crop (grass).

Natural vegetation PET with no canopy resistance (PET3) is similar to PET1, however, we assume that the canopy does not exist and therefore the windspeed is not impacted by vegetation. In this case, vegetation resistances are effectively set to zero. Albedo, aerodynamic resistance, and windspeed height are the same as for PET1.

2.2 Description of Climate Change Scenarios

In this chapter, we evaluate simulations of the VIC model under three types of climate change scenarios for the 2020s (30 year average centered on 2025), 2040s (30 year average centered on 2045), and 2080s (30 year average centered on 2085). The first type of climate change scenario is similar to that using the approach taken by Elsner *et al.* 2010, in which projected average monthly changes in precipitation and temperature are applied as perturbation factors to the historical model forcing dataset on a daily basis. This approach is often referred to as the delta method approach.

The second type of climate change scenario is typically called the transient scenario and follows the approach of Wood et al. 2004 and Salathé et al. 2007, in which GCM simulations are bias corrected and statistically downscaled to the spatial resolution of the hydrologic model (in this case VIC). The result is a daily timestep gridded dataset

for the CRB (including coastal drainages in Washington and Oregon) from approximately 2000 through 2099.

The third type of climate change scenario is introduced in this report and is a hybrid method between the delta method approach and the statistical downscaling method. In this method, GCM scenarios are spatial downscaled to the resolution of the VIC model ($1/16^{th}$ degree) and at a monthly timestep. The historical dataset at a daily timestep is aggregated to monthly timestep and bias corrected against the spatially downscaled dataset to produce a new dataset with the realistic variability of storms from the historical dataset and the climate change signals of the spatially downscaled dataset, including projected changes in climate variability and magnitude of change. For further details on the development of the three types of climate change scenarios, refer to Chapter 4 on GCM downscaling methods and applications.

2.3 Soil, Vegetation, and Snowband parameters

In addition to timeseries forcings, the VIC model uses as input four parameter files which are static and predefined: the soil parameter file, vegetation parameter file, vegetation library, and snowbands parameter file. Each parameter file contains information specific to each model grid cell, while the vegetation library contains general information for vegetation types that may be referenced by the vegetation parameter file.

The soil parameter file contains information such as soil layer, infiltration parameters and many others, which are defined by Liang *et al*. (1994 and 1996). Typical VIC model calibration parameters may be found in the soil parameter file and these include middle and bottom layer soil depths as well as parameters that define the variable infiltration capacity function. The soil parameter file developed for the $1/8^{th}$ degree VIC implementation of the PNW (Maurer *et al*. 2002) was used as a basis for the $1/16^{th}$ degree soil parameter file used in this study, although some parameters were recomputed at $1/16^{th}$ degree including average grid cell elevation, annual average air temperature, annual average precipitation, and average July temperature.

Typically, model calibration includes the assignment of a single soil layer depth across the calibrated watershed, regardless of whether the grid cell is located in a steep mountainous region or in a flat low lying floodplain. In an effort to incorporate more realistic soil depths, in this study we have fixed the top and middle soil depths to 0.1 and 0.3 meters, respectively, and applied the soil depth algorithm within the DHSVM model to calculate the soil depth of the bottom VIC model soil layer (Wigmosta *et al*. 1994). Simply, the algorithm uses a predefined soil depth range for the watershed (in this case 0.5 to 2.5 meters) and a DEM to assign a soil depth to each grid cell within this range, based on mean cell elevation and aspect (as computed from the DEM). The resulting map of total soil depth for the PNW applied in this study is provided in Figure 3.

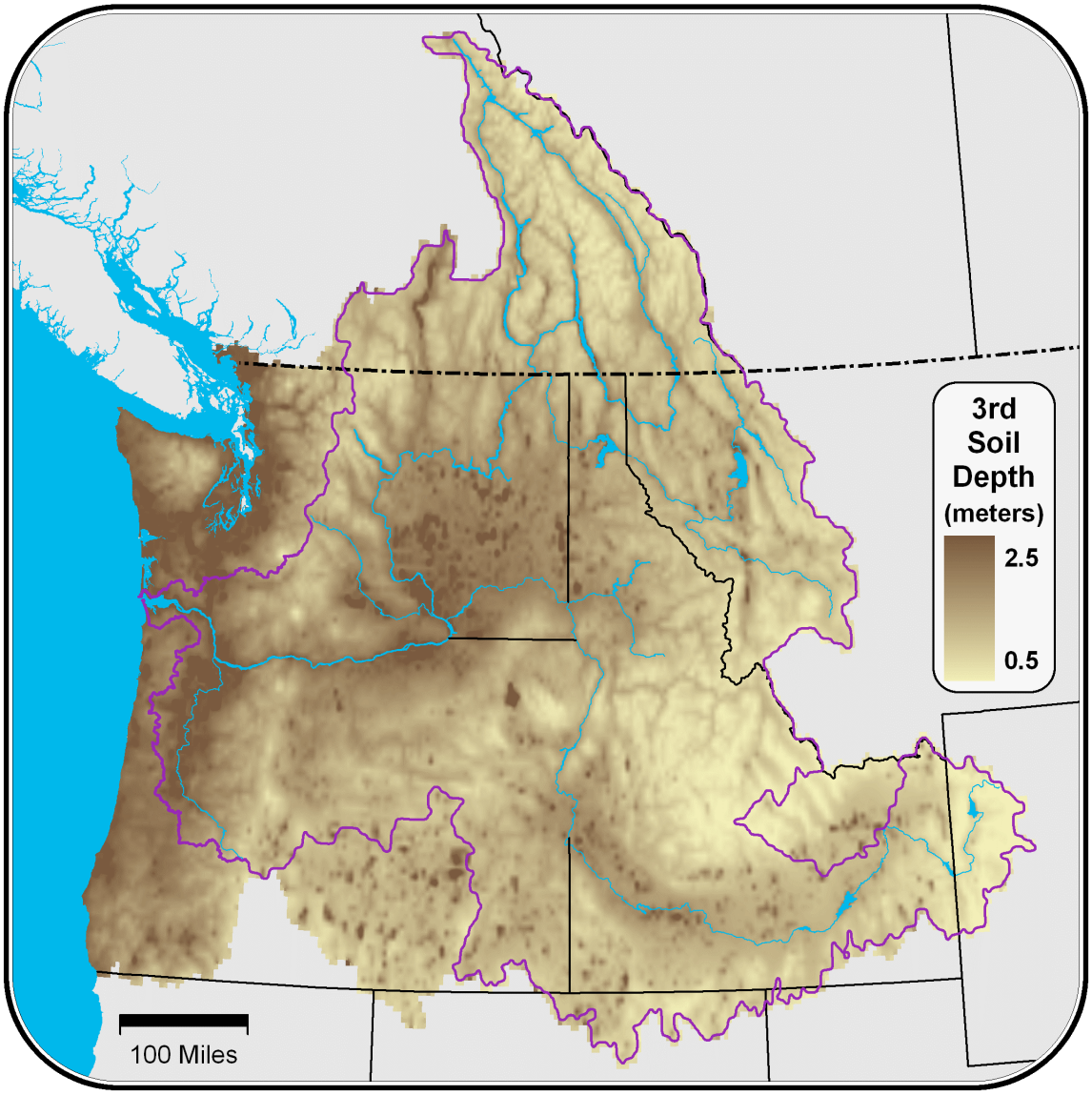

Figure 3 VIC model third (bottom) layer soil depths at 1/16th degree latitude longitude resolution.

The vegetation parameter file used in this study is based on preprocessed parameters from the LDAS (Land Data Assimilation System) dataset for the continental United States, which utilizes a vegetation classification scheme from the University of Maryland (UMD) (Hansen *et al.* 2000) at 1 km spatial resolution. Vegetation data at this scale were aggregated to produce vegetation parameters at 1/16th degree resolution. The vegetation library is also based on the UMD classification scheme.

The snowbands parameter file includes the definition of elevation bands within each VIC model grid cell. The number of elevation bands assigned for a grid cell is based on two criteria, namely a band may not have a maximum elevation range of more than 500 meters, with a maximum of 5 elevation bands per grid cell. For those cells where more that 5 bands would be required to accommodate the 500 meter range limit, the number of bands is set to 5 and the elevation ranges are equally distributed between them. Elevation bands are determined based on a 30 arcsecond (or approximately 1km) DEM.

2.4 Application of off-line streamflow routing model and routing network

As mentioned in section 2.1, the VIC model produces runoff and baseflow at each model grid cell for each model timestep. An off-line, or separate streamflow routing model, developed by Lohmann *et al.* (1996), computes streamflow at chosen locations based on convolution of runoff and baseflow. A predetermined routing network provides the upstream-downstream linkage between VIC model grid cells.

The routing network was developed based on the 30 arcsecond digital elevation model (DEM) from the U.S. Geological Survey (USGS) for the continental US (http://eros.usgs.gov/ - /Find_Data/Products_and_Data_Available/gtopo30/hydro). A 1km digital streamflow layer was imprinted or "burned" into the DEM to clearly mark stream channels into the DEM (http://eros.usgs.gov/ - /Find_Data/Products_and_Data_Available/gtopo30/hydro). Further processing steps using built in tools in ArcGIS Desktop were applied to develop the streamflow routing network at 1/16th degree spatial resolution to exactly match the resolution of the VIC model.

The 297 streamflow routing locations described in Chapter 3 (this report) were then located on the developed streamflow routing network and verified based on their true latitude-longitude location. Adjustments were made to streamflow site locations if the computed upstream watersheds area using the routing network was not within 10% of the cited watershed area by the USGS.

2.5 Model calibration

Calibration of the VIC hydrologic model was conducted using a similar approach to Matheussen *et al*. (2000), in which major sub-watersheds of the CRB were identified and routed streamflow at the sub-watershed outlets were calibrated on a monthly timestep to available natural (or unregulated) streamflow data. Calibration watersheds as well as model calibration and validation statistics are provided in Table 2 and error statistics include Nash Sutcliffe efficiencies (NSE) and R^2. A well calibrated model typically yields a NSE and R^2 higher than 0.7 (Liang *et al.* 1996; Nijssen *et al*. 1997).

Table 2 Summary monthly error statistics for VIC model calibration for 12 major watersheds.

Basins (gage)	**N-S model efficiency**	**R^2**
Columbia River at Revelstoke		
Calibration period (1975-1989)	0.76	0.80
Validation period (1960-1974)	0.76	0.80
Kootenay River at Corra Linn		
Calibration period (1975-1989)	0.89	0.89
Validation period (1960-1974)	0.93	0.93
Pend D'Oreille River at Waneta		
Calibration period (1975-1989)	0.88	0.91
Validation period (1960-1974)	0.85	0.93
Kootenai River at Libby		
Calibration period (1975-1989)	0.77	0.88
Validation period (1960-1974)	0.90	0.92
Columbia River at Priest Rapids		
Calibration period (1975-1989)	0.89	0.89
Validation period (1960-1974)	0.91	0.92
Yakima River at Parker		
Calibration period (1975-1989)	0.78	0.84
Validation period (1960-1974)	0.80	0.85

Clearwater River at Dworshak		
Calibration period (1975-1989)	0.77	0.82
Validation period (1960-1974)	0.68	0.86
Snake River at Milner		
Calibration period (1975-1989)	0.74	0.82
Validation period (1960-1974)	0.77	0.78
Columbia River at Ice Harbor		
Calibration period (1975-1989)	0.83	0.90
Validation period (1960-1974)	0.93	0.94
Willamette River at Portland		
Calibration period (1975-1989)	0.89	0.93
Validation period (1960-1974)	0.91	0.93
Columbia River at The Dalles		
Calibration period (1975-1989)	0.89	0.90
Validation period (1960-1974)	0.92	0.92

VIC model calibration was conducted using an autocalibration tool called MOCOM-UA developed by the Land Surface Hydrology group at the University of Washington, following the approach of Yapo *et al*. (1998). The code was improved upon by the Pacific Climate Impacts Consortium at the University of Victoria, British Columbia. This tool uses a multi-objective function and shuffle complex evolution procedure to optimize model calibration parameters to create a set of pareto (equally) optimal calibration parameters. The user may define the number of calibration parameters, the number of objectives on which to perform optimization, and the error statistics on which to base the objective function. The calibration implementation approach taken for this study includes 50 initial parameter sets to define the optimization parameter space, 25 parameter sets which advance forward in each evolution of optimization, 3 VIC model calibration parameters including Ds, Dsmax, and Ws, and 6 error statistics which define the multiple objective function: r^2, NSE, the logarithm of the NSE, annual volume error, mean hydrograph peak difference, route mean squared error (RMSE), and number of sign changes when subtracting the simulated monthly

hydrograph from the observed natural hydrograph. The optimization function can be generally stated by the following relationship:

Min F = {-NSE(Q), -logNSE(Q), VolErr(Q), -R2(Q), PeakDiff(Q), RMSE(Q), NumSC(Q)}

Where,

NSE(Q) = Nash Suttcliffe Efficiency
logNSE(Q) = logarithm of Nash Suttcliffe Efficiency
VolErr(Q) = annual volume error (in 1000AF)
R2(Q) = r^2
Peak Diff(Q) = mean hydrograph peak difference
RMSE(Q) = rout mean squared error
NumSC(Q) = number of sign changes

Model calibration used a split sample approach in which calibration was performed for each of the 11 primary watersheds over a 15 year period (typically water years 1975-1989) and model validation was performed over a separate 15 year period (typically water years 1960-1974). Calibration and validation periods were chosen to include a range of streamflow conditions with which to test model performance. Other parameters (e.g. simulated SWE or soil moisture) were not used to further constrain model parameters. However, previous studies comparing VIC simulated SWE with observations (Andreadis *et al.* 2009) and soil moisture with observations (Maurer et al. 2002; Mote *et al*. 2005)), indicate that the model successfully simulates grid level processes that are appropriately sensitive to climate forcing and other factors.

Model calibration parameters were further validated at smaller watershed scales where naturalized flow data were available. Results of model calibration and validation are presented in Section 1.5.

A number of calibrations tests were performed prior to calibration to inform and help refine the process. For example, a test run of the Yakima basin with and without use of the variable soil depth map indicated that map caused a decrease in the Nash Suttcliffe Efficiency (0.71 down to 0.57) and RMSE values (114.9 up to 133.2 kaf). The coefficient of determination, R^2, did not change (0.94).

Additional test runs were performed on the Naches watershed, a subbasin of the Yakima River basin, to investigate whether calibration of multiple parameters simultaneously is advantageous over successive calibrations where certain parameters are calibrated then fixed while additional parameters are calibrated. Specifically, we tested the impact of 1) calibrating first the infiltration parameters (bi, Ds, Dsmax, and Ws) and subsequently the bottom soil layer depth as well as 2) the impacts of calibrating all 5 parameters simultaneously. We found the results Nash Suttcliffe Efficiencies and RMSE were the same (0.56 and 54.6kaf, respectively), while the R^2 was improved in test (2) over (1), with values of 0.75 and 0.67, respectively. Although this test did not include all scenarios, it did indicate that similar error statistics may be gained through both approaches and autocalibration run time is highly dependent on the number of parameters to be optimized. Successive calibrations with a smaller parameter space may prove to be a significant long-term time savings. Further testing is needed to evaluate this hypothesis.

Non-parametric, statistical bias correction techniques (Snover *et al*. 2003) have also been employed at sites for which naturalized or modified flow was available to remove systematic bias from the streamflow simulations. These approaches provide an alternative to traditional calibration techniques (such as described above) and are particularly effective when errors in the hydrologic simulations are likely to be related to errors in meteorological driving data sets (a frequent occurrence at relatively small spatial scales). Chapter 8 describes these data processing steps in greater detail.

2.6 Basin Scale Model Evaluation

VIC model calibration was conducted over 11 subbasins of the Columbia River as described in Section 1.4 and illustrated in Figure 1. The time period used for calibration was water year 1975 to 1989 (October 1974 through September 1989). This 15 year period encompasses a range of wet, dry, and average years to test VIC model performance under these conditions. A separate 15 year period was used for model validation, namely water year 1960 to 1974 (October 1959 through September 1974). This period also encompasses a range of climatic and streamflow conditions under which we can evaluate VIC model performance. Error statistics used to test model performance included Nash-Sutcliffe efficiency, the logarithm of the Nash-Sutcliff efficiency, annual volume error, R^2, mean hydrograph peak difference, route mean squared error (RMSE), and number of sign changes. The NSE and R^2 reflect the ability of the VIC model to simulate proper magnitude and timing of streamflow without influence from existing model bias. For this reason, these statistics for each site for which observed natural streamflow was available are illustrated in Figure 4. In the figure, the larger points represent those primary sites that were used for model calibration and validation.

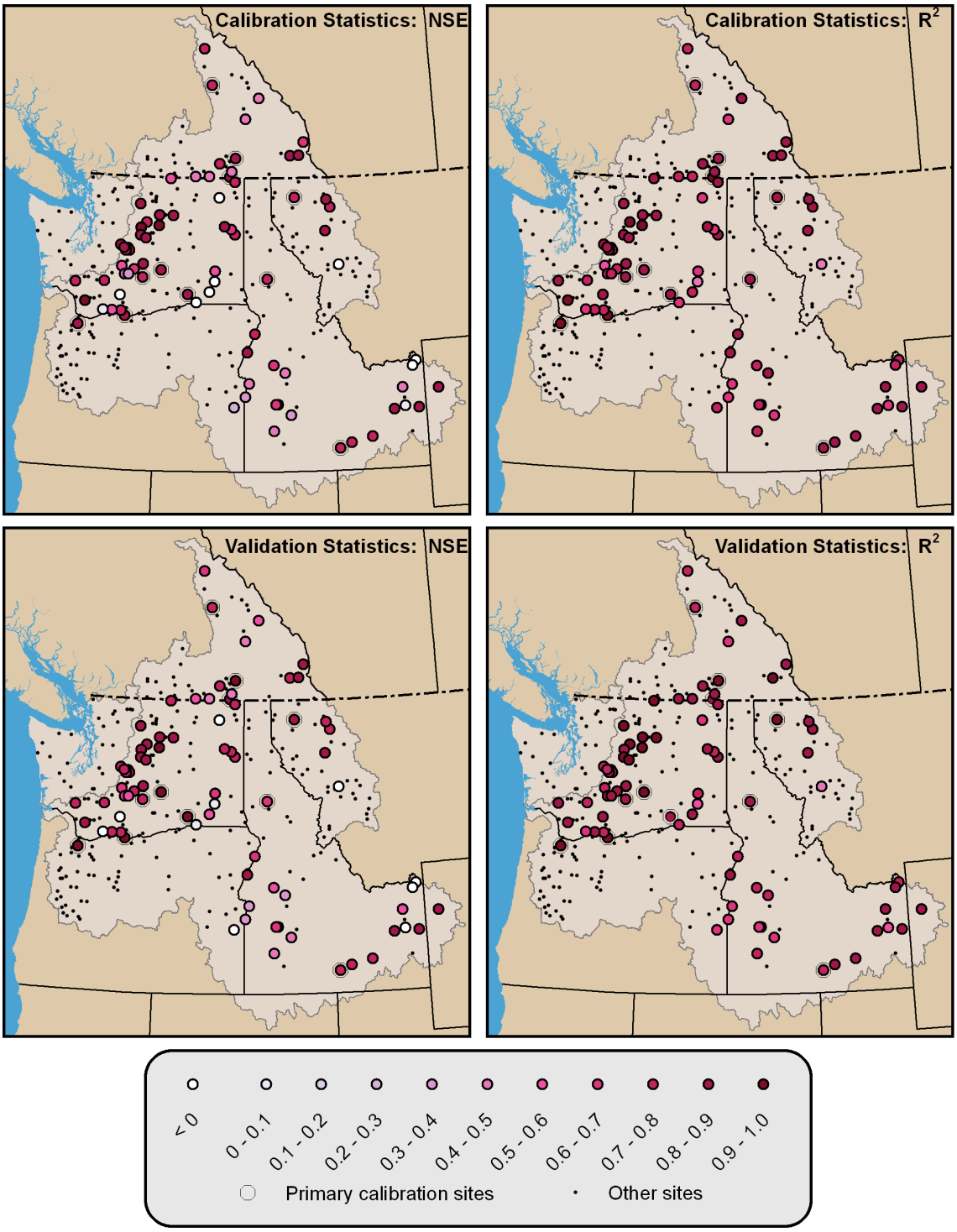

Figure 4 Summary map of 80 of the total 297 streamflow locations where error statistics between simulated and naturalized flow were computed. The top two panels show the Nash Sutcliffe Efficiency (left) and R2 (right) for the calibration period, while the two lower panels show Nash Sutcliffe Efficiency (left) and R2 (right) for the validation period. Small black dots indicate those sites where naturalized flows were not available.

We assume that VIC model calibration parameters determined for 11 major subbasins of the Columbia River are appropriate for all subbasins within them. However, we might expect that smaller subbasins have different hydrologic characteristics than the large watershed that contains it and therefore would require unique calibration parameters for proper simulation. We did a test of three subbasins of the WANET basin (Pend Oreille River at Waneta Dam): BLAGA (Little Blackfoot River near Garrison), SWANR (Swan River near Big Fork), and BITWF (W Fork Bitterroot River near Conner). NSE and R^2 parameters for the calibration parameters at WANET are 0.879 and 0.910, respectively.

Table 3 summaries these error statistics for the three subwatersheds using two sets of calibration parameters: those using the WANET calibration parameters and those determined through independent calibration of the three watersheds. For these subbasins, there is little improvement in error statistics through calibration of small watersheds independently and additionally, the time savings in model calibration time help to justify use of calibration parameters at larger scales. In the case of the WANET basin, the calibration of this watershed is complicated by possible bias in meteorological data (as implied by less than ideal calibration error statistics), which would limit calibration success potential for subwatersheds within it. Potential biases in meteorological data are generally not compensated by adjusting calibration parameters.

Table 3 Comparison of error statistics (NSE and R^2) for three subbasins of the WANET calibration basin. Top set of statistics use WANET calibration parameters, while the lower set uses independent calibration parameters for each subbasin.

Sub-basin	**SWANR**	**BLAGA**	**BITWF**
Calibration Parameters	Ds=0.375 Ws=0.872 Dsmax=2.298	Ds=0.375 Ws=0.872 Dsmax=2.298	Ds=0.375 Ws=0.872 Dsmax=2.298
NSE	0.780	0.487	0.577
R^2	0.801	0.640	0.666

Calibration Parameters	Ds=0.543 Ws=0.963 Dsmax=5.514	Ds=0.017 Ws=0.347 Dsmax=6.788	Ds=0.363 Ws=0.434 Dsmax=1.254
NSE	0.827	0.559	0.579
R^2	0.837	0.643	0.657

3. Key Findings/Discussion

Although predictions of changes in winter precipitation over the PNW have differed somewhat among recent IPCC reports (the 1995 report suggests an increase, whereas the 2001 report indicates only modest changes and the 2007 report indicates increases of a few percent by the 2040s and up to 8 percent by the 2080s, compared with the 1970-1999 climatological mean), warmer temperatures in all previous assessments have led to projections of reduced snowpack, and transformation of sensitive watersheds from being fed by a mix of rain and snow to predominantly rain. Other impacts common to previous studies of hydrological impacts of climate change in the PNW include earlier spring peak flow and lower summer flows. A wide range of hydrologic products are available on the project web site (http://www.hydro.washington.edu/2860/), as described in Chapter 7, 8 and 9, but we provide an overview of some key hydrologic impacts over the entire CRB.

3.1 Snowpack and streamflow

The PNW is typically characterized as having three representative types of watersheds, dictated mainly by the form of precipitation they receive throughout the year. These include rain dominant watersheds, were most annual precipitation falls as rain; transient watersheds, where annual precipitation is a mix of rain and snow; and, snow dominant, where a majority of annual precipitation falls as snow in the cool season. Figure 5 illustrates this classification through the metric of the ratio of peak snow water equivalent to October through March precipitation. This metric is further described in Elsner *et al*. 2010. Generally, lower elevation coastal watersheds are classified as rain dominant, while watersheds in the headwaters of the Columbia River basin are classified as snow dominant. Much of the interior Columbia basin consists of mid-elevation transient watersheds. These are particularly sensitive to climate change because small

changes in temperature can significantly change the balance of precipitation falling as snow versus rain.

Using traditional delta method climate change scenarios, we illustrate how projected changes in precipitation and temperature are likely to impact snowpack in the PNW, and thus alter the rain/snow balance. Figure 6 illustrates mean projected changes in SWE on April 1 for three future time periods, the 2020s, 2040s, and 2080s, and two greenhouse gas emissions scenarios, A1B and B1. April 1 SWE is a common indicator of summer water supply in the PNW and is therefore a useful metric for evaluating projected change. Results show that snowpack throughout the region is likely to experience modest declines through the 2020s (compared with the historical 1916-2006 mean) of about 18%, with increasingly significant declines further into the 21st century. In general, the Canadian portion of the Columbia River basin will be less significantly impacted than the remaining parts of the basin. Also, due to its assumption of higher future greenhouse gas emissions, the A1B scenario generally indicates greater impacts to hydrology than the B1 scenario.

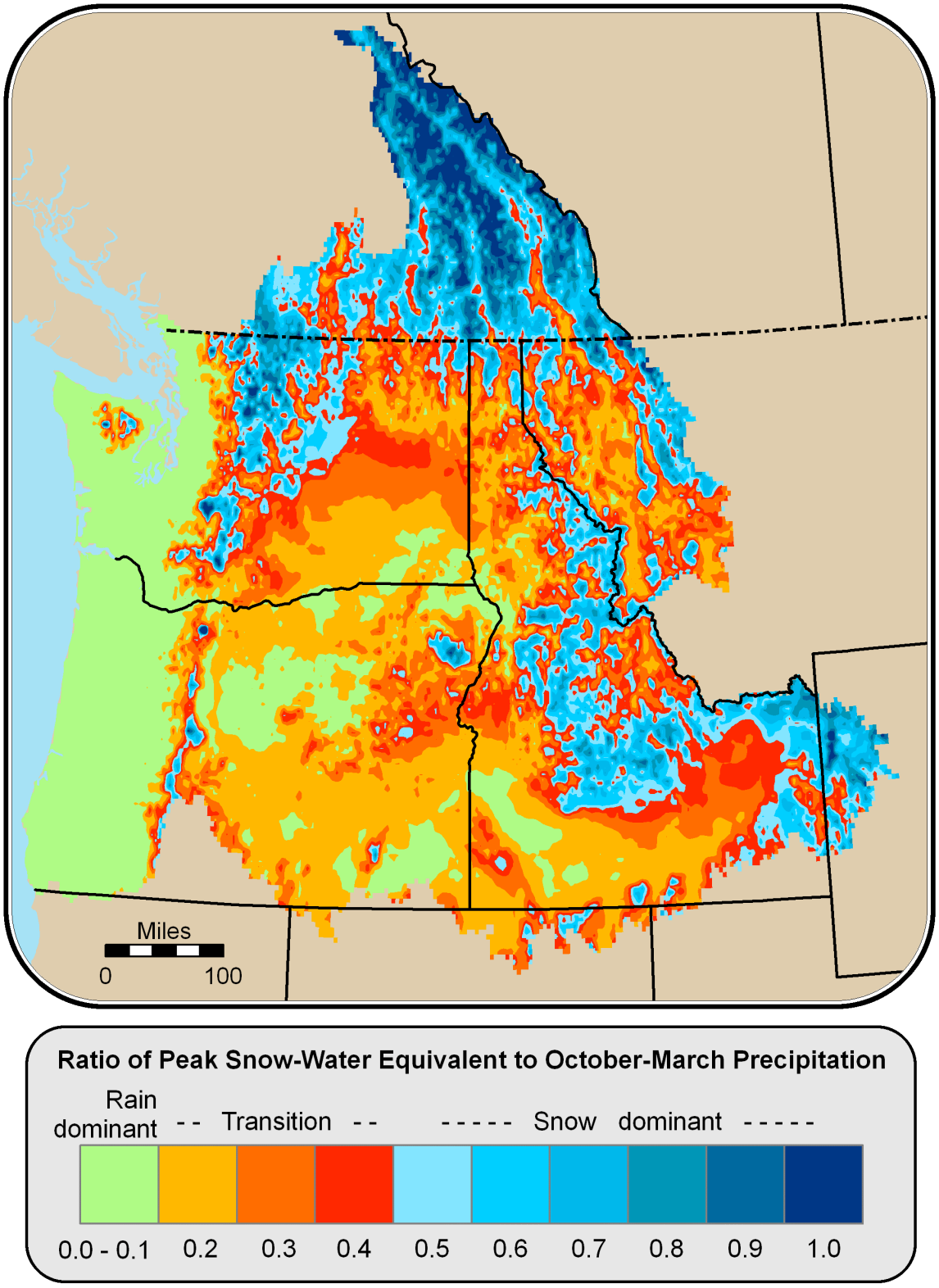

Figure 5 The average ratio of peak VIC model simulated snow water equivalent (SWE) to October – March precipitation for the historical period (water year 1917-2006)

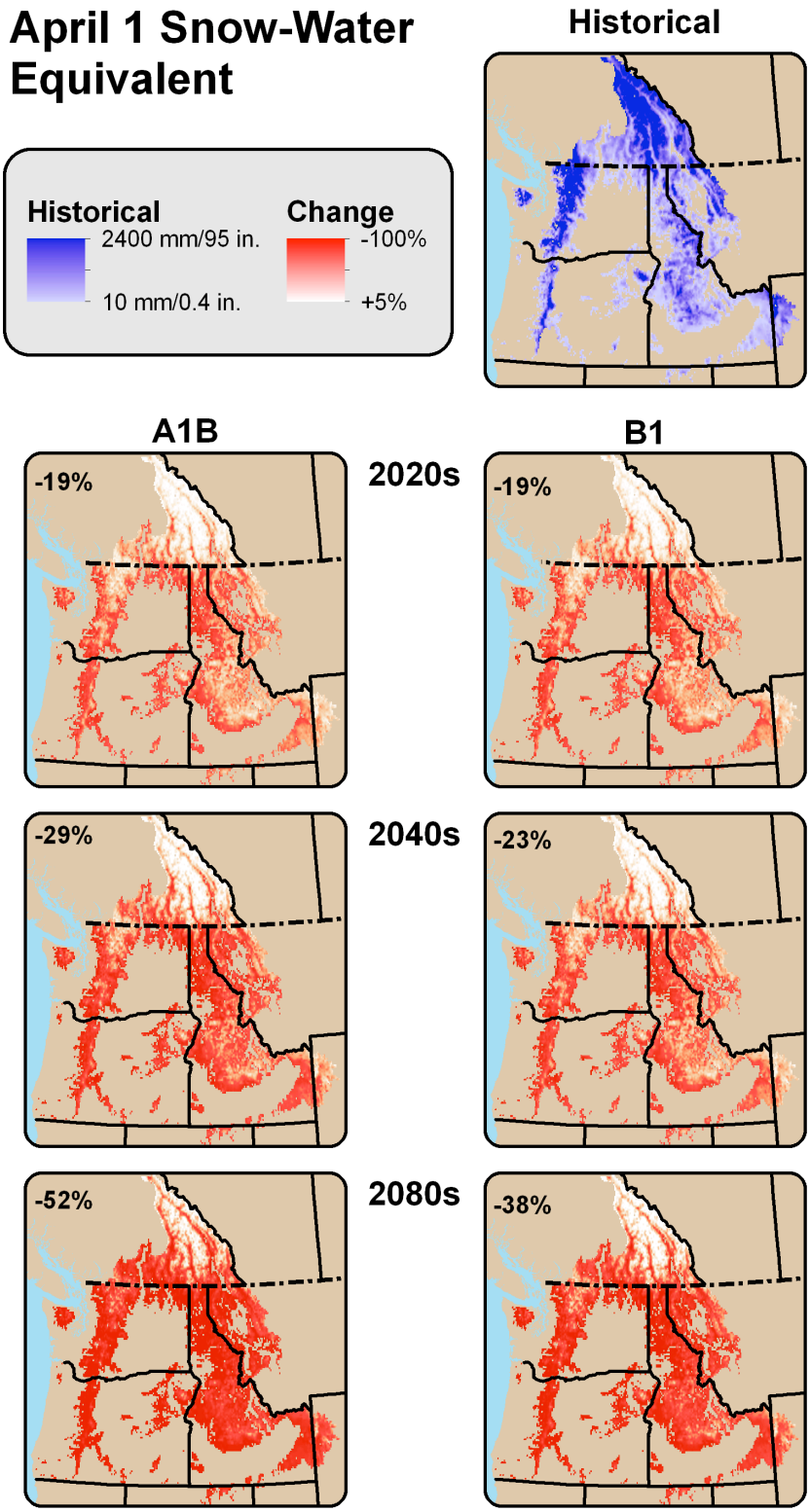

Figure 6 Summary of historical (mean 1916-2006 water years) April 1 snow water equivalent and percent (%) changes in April 1 snow water equivalent projected using A1B (left) and B1 (right) emissions scenarios for the 2020s, 2040s, and 2080s compared with historical. Domain average percent change is reported in the upper left corner of each figure panel.

Significant declines in snowpack have important implications for regional streamflow, as illustrated by Figures 7 and 8. Figure 7 illustrates mean historical (water year 1916-2006) and mean projected runoff hydrographs using the hybrid delta method approach for the 2040s for three sites: the Columbia River at the Dalles, the Snake River at Milner, and the Yakima River at Parker. Similar to figure 7, figure 8 summarizes results from the transient climate change scenarios for the same three basins and future time period. Runoff presented in these figure represents mean flow across the watersheds and has not been routed through stream channels. Still, these hydrographs are illustrative of the changes in streamflow volume and timing projected for the 2040s at these sites. The Columbia River as a whole and the Snake River above Milner dam may be considered as snow dominant watersheds because runoff generally peaks in late spring as snowmelt is the main contributor to runoff. In the 2040s for these watersheds, both hybrid delta and transient scenarios project modest increases in winter flow, decreases in summer flow, as well as a shift in the peak of the hydrographs earlier in the season. The range of transient scenario projections is generally tighter than the hybrid delta method scenario projections. In part, this reflects the smaller number of transient projection ensembles (7), compared with hybrid delta projection ensembles (10). Furthermore, the 7 best GCMs were chosen for the transient scenarios, based on their ability to reproduce 20th century climate (refer to Chapter 4), while the 10 best were chosen for the hybrid delta scenarios.

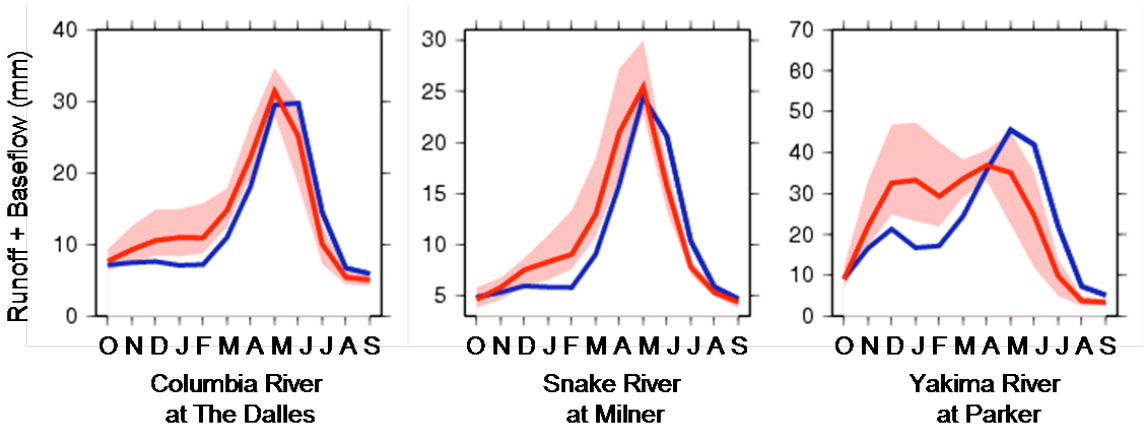

Figure 7 Projected combined flow (runoff + baseflow) in millimeters for the 2040s A1B scenario at three sites in the Columbia River basin. The blue line represents the historic monthly mean flow (water years 1916-2006) while the red line represents projected monthly mean flow averaged across 10 A1B hybrid delta method scenarios for the 2040s (representing mean 2030-2059 climate). The red band represents the range of projections from the 10 individual A1B hybrid delta method scenarios.

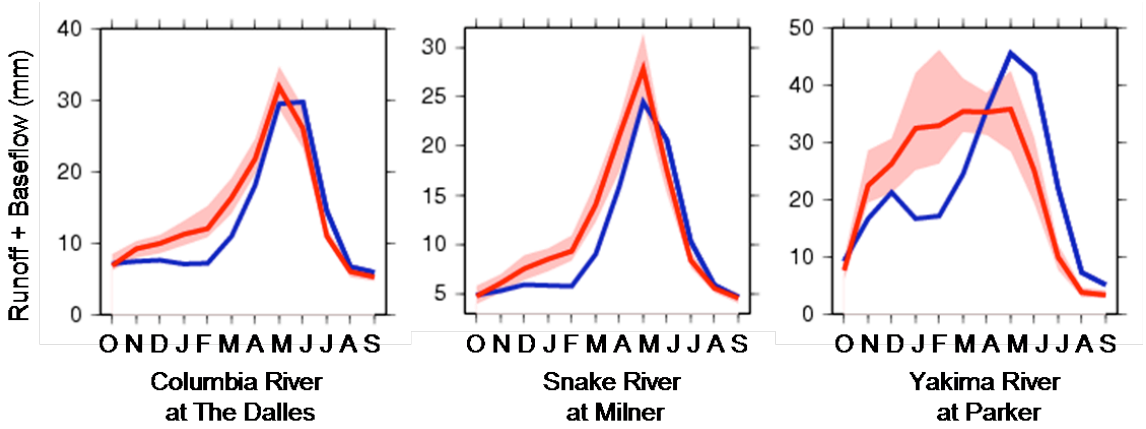

Figure 8 Projected combined flow (runoff + baseflow) in millimeters for the 2040s A1B scenario at three sites in the Columbia River basin. The blue line represents the historic monthly mean flow (water years 1916-2006) while the red line represents projected monthly mean flow averaged across 7 A1B transient scenarios for the 2040s (representing mean 2030-2059 climate). The red band represents the range of projections from the 7 individual A1B hybrid delta method scenarios.

3.2 Potential and actual evapotranspiration

Figure 9 summarizes mean historical (1916-2006) summer PET (average sum of June, July, and August) and percent change in projected summer PET for the 2020s, 2040s and 2080s using A1B and B1 emissions scenarios and the traditional delta method approach. Historically, average summer PET ranges from 130 to 630mm, with higher PET in southeastern Oregon and east of the Cascade mountains. The western flanks of the Cascades and the interior Columbia and Snake basins have modest to lower PET, while south central Oregon has the lowest PET in the region. These variations in PET across the region appear to be largely dependent on vegetation type. Regions with lowest summer PET historically are typically classified as shrublands, while regions with highest summer PET historically include wooded areas, both deciduous and evergreen.

Projected changes in average summer PET show growing summer PET in the coastal and mountainous parts of the domain and no change to decreases in PET in the interior Columbia and interior Snake basins. The magnitudes of these changes increase (in both positive and negative directions) further into the future and impacts using A1B scenarios are generally more significant than those using B1 scenarios. Increases PET are driven mainly by increases in VPT (vapor pressure deficit), while decreases in PET are driven mainly by increases in outgoing longwave radiation due to projected temperature change and higher albedo of shrubland and cropland vegetation.

Figure 10 summarizes mean historical (1916-2006) summer AET (average sum of June, July, and August) and percent change in projected summer AET for the 2020s, 2040s, and 2080s using A1B and B1 emissions scenarios and the traditional delta method approach. Historically, mean summer AET ranges from 24mm to 440mm for the PNW, with the greatest AET occurring along the coast and mountainous parts of the region. The lowest AET occurs in the interior Columbia basin, central Oregon, and the interior Snake River basin. Regions if higher AET closely correspond with the forested parts of the region.

Projected AET is likely to increase in western Washington and along windward slopes of the mountain ranges and decrease in most of the other parts of the PNW, in particular on the leeward slopes of the mountain ranges. The magnitude of these changes is projected to increase further into the future and A1B scenarios generally indicate greater changes than the B1 scenarios. Decreases in AET over much of the region correspond with overall decreases in summer precipitation. Despite decreases in summer precipitation, the mountains are projected to experience increases in AET which is likely due to increased water availability through enhanced snowmelt and increased soil moisture.

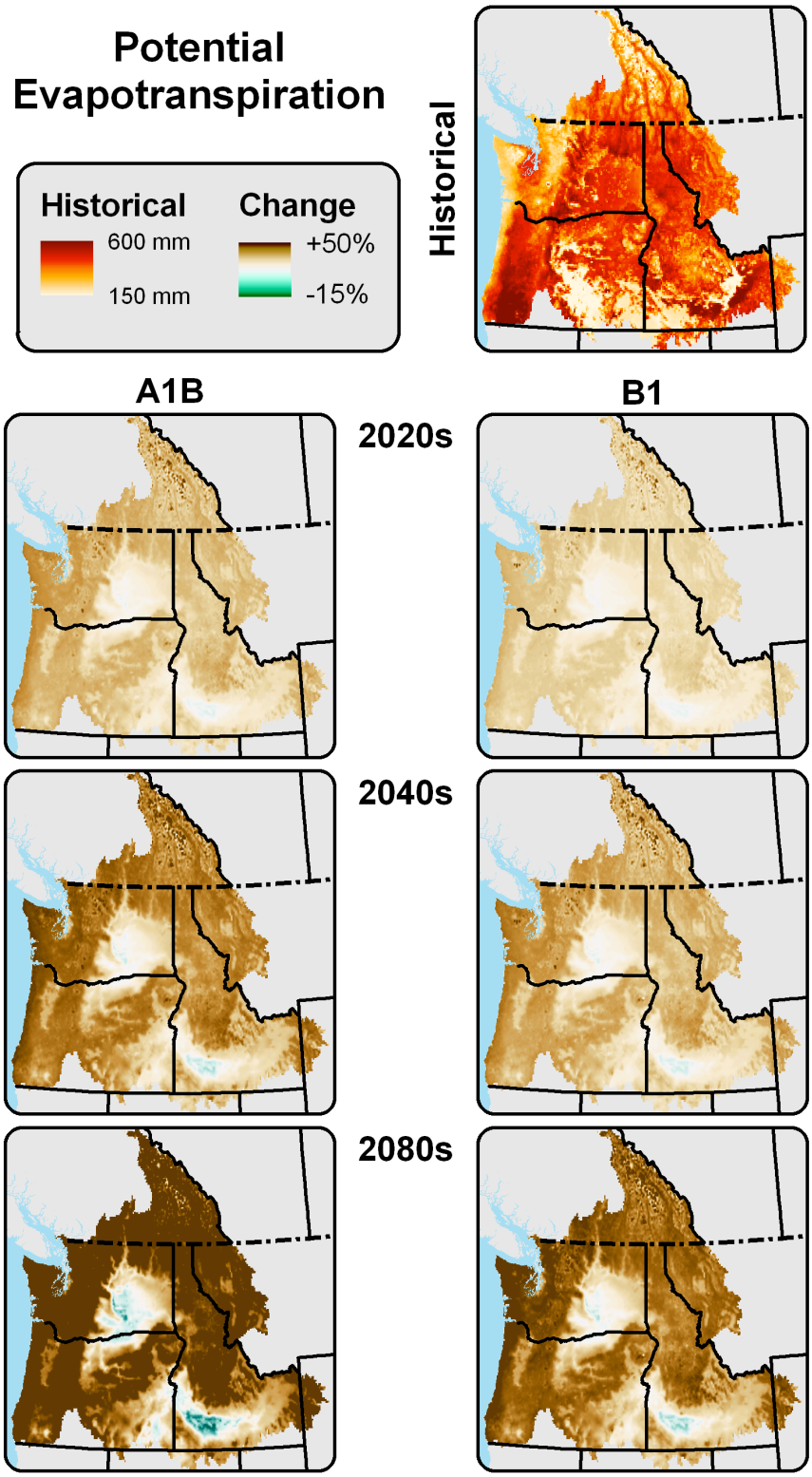

Figure 9 Summary of historical (mean 1916-2006 water years) total summer (July, August, September) potential evapotranspiration and percent (%) changes in summer potential evapotranspiration projected using A1B (left) and B1 (right) emissions scenarios for the 2020s, 2040s, and 2080s compared with historical.

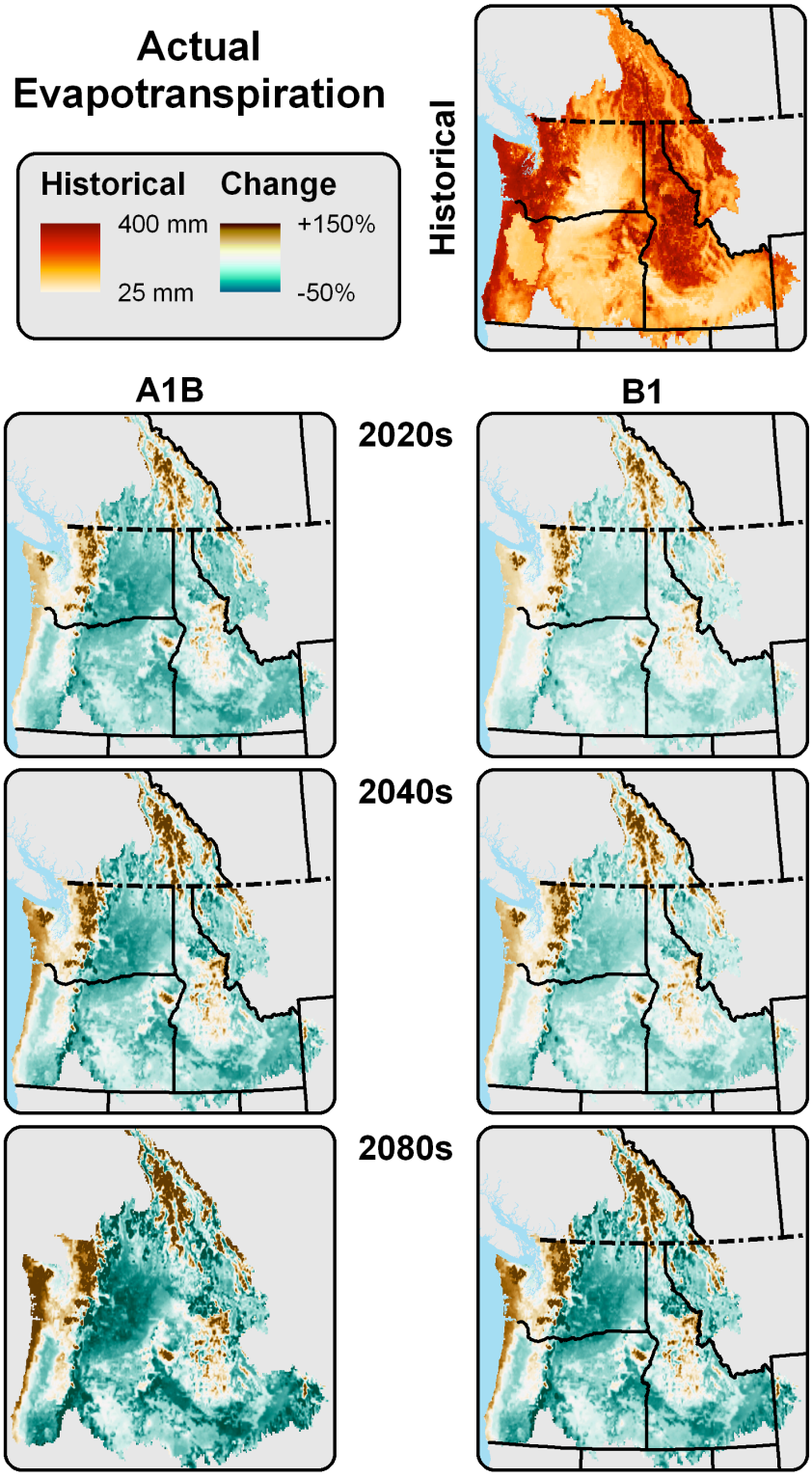

Figure 10 Summary of historical (mean 1916-2006 water years) total summer (July, August, September) evapotranspiration and percent (%) changes in summer evapotranspiration projected using A1B (left) and B1 (right) emissions scenarios for the 2020s, 2040s, and 2080s compared with historical.

4. Conclusions

The VIC macroscale hydrologic model was calibrated and implemented at 1/16th degree spatial resolution over the greater Columbia River basin (Columbia River watershed plus coastal drainages in Washington and Oregon) for historical period 1915-2006 and three types of projected climate change scenarios. These scenarios include 19 hybrid delta scenarios (10 for A1B and 9 for B1 greenhouse gas emissions scenarios) for three future time periods, 2020s, 2040s, and 2080s; 14 statistically downscaled continuous transient simulations for generally 1950-2099 (7 for A1B and 7 for B1); and, 2 composite delta method scenarios for the 2020s, 2040s, and 2080s (1 for A1B and 1 for B1).

In this chapter, we summarized our methodology for model calibration and validation; we described additional output variables offered through this implementation (namely five forms of PET) and array of climate change scenarios available; and, finally we summarized some of the key information available through this study, which is now available through an online database. The results illustrate that climate change is significantly affecting the water resources in the Columbia River watershed and will continue to do so through this century. Reduced winter snowpack and changes in the timing and availability of water to plants and streams have implications across many sectors. The datasets we provide offer a common set of tools which are a useful tool for evaluating impacts as part of independent regional climate change studies.

5. References

Andreadis K, Storck P, and Lettenmaier DP (2009) *Modeling snow accumulation and ablation processes in forested environments,* Water Resources Research, 45, W05429, doi:10.1029/2008WR007042.

Cherkauer KA and Lettenmaier DP (2003) *Simulation of spatial variability in snow and frozen soil field,* J. Geophy. Res. Vol. 108, No. D22, 8858-, doi:10.1029/2003JD003575

Elsner MM, Cuo L, Voisin N, Deems JS, Hamlet AF, Vano J, Mickelson KEB, Lee SY, Lettenmaier DP (2010) *Implications of 21st Century climate change for the hydrology of Washington State,* Climatic Change DOI:10.1007/s10584-010-9855-0.

Hamlet AF, Lettenmaier DP (1999*) Effects of climate change on hydrology and water resources of the Columbia River basin*, J Am Water Resour Assoc 35:1597–1624

Hamlet AF, Lee SY, Mickelson KEB, Elsner MM (2010) *Effects of projected climate change on energy supply and demand in the Pacific Northwest and Washington State,* Climatic Change, DOI: 10.1007/s10584-010-9857-y.

Hansen, MC, DeFries RS, Townshend JRG and Sohlberg R (2000) *Global land cover classification at 1km spatial resolution using a classification tree approach*, International Journal of Remote Sensing, 21, 1331-1364, 2000.

IPCC (2007) Summary for policymakers. In: *Climate Change 2007: The physical science basis. Contribution of working group I to the fourth assessment report of the intergovernmental panel on climate change*. Solomon S, Qin D, Manning M, Chen Z, Marquis M, Averyt KB, Tignor M Miller HL (eds) Cambridge University Press, Cambridge, United Kingdom and New York, NY, USA

Lee SY, Hamlet AF, Fitzgerald CJ, and Burges SJ (2009) *Optimized Flood Control in the Columbia River Basin for a Global Warming Scenario*, Journal of Water Resources Planning and Management, DOI 10.1061/(ASCE)0733-9496(2009)135:6(440), 135(6) 440-450

Liang X, Lettenmaier DP, Wood EF, Burges SJ (1994*) A simple hydrologically based model of land surface water and energy fluxes for GSMs*. J Geophys Res (99)D7: 14,415-14,428

Liang X, Wood EF, Lettenmaier DP (1996) *Surface soil moisture parameterization of the VIC-2L model: Evaluation and modifications*. Glob Planet Chang 13: 195-206

Liang X, Wood EF, Lohmann D, Lettenmaier DP, and others (1998) *The project for intercomparison of land-surface parameterization schemes (PILPS) phase-2c Red-Arkansas River basin experiment: 2. Spatial and temporal analysis of energy fluxes*, J Glob Planet Chang 19: 137-159

Littell, J.S., E.E. Oneil, D. McKenzie, J.A. Hicke, J.A. Lutz, R.A. Norheim, and M.M. Elsner. (2010). *Forest ecosystems, disturbance, and climatic change in Washington State, USA*. Climatic Change, DOI: 10.1007/s10584-010-9858-x

Lohmann, D., Nolte-Holube, R. and Raschke, E., (1996) *A large scale horizontal routing model to be coupled to land surface parameterization schemes*. Tellus **48 A**, pp. 708–72

Maidment, D. R., ed., (1993) "*Handbook of Hydrology*," McGraw-Hill.

Matheussen B, Kirschbaum RL, Goodman IA, O'Donnell GM, Lettenmaier DP (2000) *Effects of land cover change on streamflow in the interior Columbia basin*. Hydrol Proc 14(5): 867-885

Maurer, E. P., A. W. Wood, J. C. Adam, D. P. Lettenmaier, and B. Nijssen, (2002) *A long-term hydrologically based dataset of land surface fluxes and states for the conterminous United States*. J. Climate, **15**:3237–3251

Mote PW, Hamlet AF, Clark M, Lettenmaier DP (2005) *Declining mountain snowpack in western North America,* Bull Am Meteorol Soc 86(1): 39-49

Nijssen, B., D. P. Lettenmaier, X. Liang, S. W. Wetzel, and E. F. Wood (1997) *Streamflow simulation for continental-scale river basins*. Water Resour. Res, **33**, 711-724.

Payne JT, Wood AW, Hamlet AF, Palmer RN, Lettenmaier DP (2004) *Mitigating the effects of climate change on the water resources of the Columbia River basin,* Clim Change 62:233–256

Salathé, E.P., P.W. Mote, and M.W. Wiley (2007) *Review of scenario selection and downscaling methods for the assessment of climate change impacts on hydrology in the United States Pacific Northwest,* International Journal of Climatology 27(12): 1611-1621, DOI: 10.1002/joc.1540

Snover AK, Hamlet AF, Lettenmaier DP (2003) *Climate change scenarios for water planning studies: Pilot applications in the Pacific Northwest*. Bull Am Meteorol Soc 84(11):1513-1518

Vano, J.A., M. Scott, N. Voisin, C.O. Stöckle, A.F. Hamlet, K.E.B. Mickelson, M.M. Elsner, D.P. Lettenmaier (2010) *Climate change impacts on water management and irrigated agriculture in the Yakima River basin, Washington, USA*. Washington State Climatic Change. DOI: 10.1007/s10584-010-9856-z.

Wigmosta, M. S., L. W. Vail, and D. P. Lettenmaier (1994) *A distributed hydrology-vegetation model for complex terrain,* Water Resour. Res., **30**:1665–1679

Wood, A.W., L.R. Leung, V. Sridhar and D.P. Lettenmaier (2004) *Hydrologic implications of dynamical and statistical approaches to downscaling climate model outputs*, Climatic Change Vol. 62, Issue 1-3, 189-216, January.

Yapo, P. O., H. V. Gupta, and S. Sorooshian (1998) *Multi-objective global optimization for hydrological models,* J. Hydrol., **204**:83–97